ENVIRONMENTAL SEM IN WOOL RESEARCH
- PRESENT STATE OF THE ART

G.D. Danilatos and J.H. Brooks

CSIRO Division of Textile Physics,
338 Blaxland Road, Ryde, NSW,
Australia.

SYNOPSIS

The new technique of environmental SEM has been developed to a highly efficient operational state. It has been used to study greasy wool fibres treated and untreated, wet and dry, to study mechanical properties in situ and to observe liquid spreading on the fibre surface. An examination of the effect of the electron beam has been undertaken under various irradiation and environmental conditions.

INTRODUCTION

The aim of this report is to present an overview of the current uses of the environmental scanning electron microscope (ESEM) as a new tool in wool research.

The ESEM is a form of an electron microscope which allows the examination of the natural surface of materials in the presence of gases or liquids. The specimens do not have to be treated with antistatic agents or metallized. This capacity makes it suitable for studies of wool in a variety of ways. Several of these ways have been explored and the results will be reported in detail separately. At present, a brief summary of some of these applications is given with a view to addressing the interests of a wider group of researchers.

The basic principles of ESEM were presented at the previous conference[1] but the technique, after various phases of development[2-5], can now be used with superior performance. These developments were necessitated by the need to improve the contrast and resolution for the unstained wool fibres, to increase the amount of information detected by signal processing, and to construct fibre manipulative devices for experiments in situ.

EXPERIMENTAL

The fundamental task in the design and construction of an ESEM is to be able to admit gases and liquids around the specimen without significant electron beam spread and loss of signal detection. This is achieved by separating the vacuum of the electron optics from the high pressure of the specimen chamber by means of two apertures. One of these apertures can coincide with the aperture of the objective lens, whilst the second aperture is placed at the correct distance below the first one and acts as the main pressure limiting aperture. The gas that flows through the pressure limiting aperture is pumped away by suitable means before it leaks into the electron optics column. The electron beam can travel unhindered in the electron optics column, passes through the two apertures with negligible scattering and enters the high pressure region where it suffers severe scattering by the gas molecules. However, there is a useful region immediately below the pressure limiting aperture where the beam scattering and the spot broadening can be considered negligible, and this is where the specimen is placed and examined.

The modification has been achieved by suitable electron collectors capable of detecting efficiently the signals which are generated from the beam-specimen interaction. Two scintillator-type backscattered electron detectors have been installed symmetrically. This design allows optimum detection, versatility of signal processing and space to introduce sizeable fibre manipulators. The overall design details of the whole system are crucial in order to make the ESEM a realistic proposition.

When summing the outputs of the two detectors, the contrast corresponds predominantly to atomic number (Z) variation, as in Fig. 1a, apart from edge effects and gross topographic characteristics. The overall increased brightness of the treated fibre indicates a higher average Z,

probably arising from the uptake of potassium ions on the hydrolysed surface.

Fig. 1b shows the same field of view by subtracting the outputs. This is equivalent to illuminating the topography of the specimen in the direction indicated by the arrow. The undulations of the fibre surface together with the underlying adhesive tape are shown clearly. Fig. 1c shows the same field of view by inverting the difference of the outputs. In a similar fashion, any fraction of the outputs can be algebraically summed. The figures quoted on the micrographs indicate the full horizontal field width in μm.

The various parameters of the system may vary according to the conditions of operation such as the nature and pressure of gas. A typical case is to use a 400μm pressure limiting aperture with an electron beam of 10kV and 100pA in order to image an untreated wool fibre placed 1mm below the aperture at 25mbar water vapour pressure. Weaker electron beams are also possible under different conditions.

RESULTS AND DISCUSSION

1. Wetting Studies

Fig. 2a shows a droplet of water in contact with a Lincoln wool fibre. The large depth of focus and high resolution give a clear image of the contact line, not possible with light microscopy. Movement of the fibre can give an advancing or, as in Fig. 2b, receding liquid. Fig. 2c shows liquid water retained between two crossing fibres.

This work was made possible by the construction of a microinjector which allows the injection of microdroplets of various liquids in a controlled manner from ambient conditions into the hypobaric environment of the ESEM.

2. Scouring of wool

Studies of wool scouring have been assisted by the present techniques in various ways. Treated or untreated greasy fibres can be examined while changing the relative humidity (R.H.) inside the ESEM.

Degreased wool obtained by extraction with petroleum spirit only and

therefore containing suint and dirt can be seen dry in Fig. 3a. On increasing the R.H. to approximately 95%, the location of the suint was revealed by its deliquescent nature (Fig. 3b). The dirt particles are unchanged. To identify the corresponding points between the dry and wet images, the twist of the fibres must be noted. The droplets of suint solution were found adhering to every scale along the length of the fibres examined in this sample.

Fig. 4a and 4b show two portions of a greasy wool fibre from the same lot, which corresponds to a normal type fleece wool with relatively high grease and low dirt, after equilibration at 95% R.H. The suint sorbed water to form a solution, which then spread on the greasy fibre to give a smooth liquid surface. The surface of the suint solution seems to be partially covered by a scum, having a higher average Z than the suint solution. The scum may be based on calcium and magnesium salts of dicarboxylic acids; this is consistent with the Z-contrast observed. The spreading of the suint solution on the greasy fibre contrasts with its lack of spreading on the degreased fibres (Fig. 3b). This is consistent with the known hydrophobic nature of the surface of the wool fibre and points to a low interfacial tension between the suint solution and the wool grease. When the R.H. was subsequently reduced to near zero, the water evaporated to leave a thin contaminant layer revealing the scale tips (Fig. 4d) or a thick contaminant layer (Fig. 4e). Another example of the distribution of contaminants is seen on a different fleece type (dirty), first dry in Fig. 4c and then at 95% R.H. in Fig. 4f.

A time sequence of the drying of greasy fibres observed in situ in the ESEM is shown in Figs. 5a to 5f. A lump of greasy wool fibres was immersed in water for 20 minutes and then transferred wet into the microscope. The first image (Fig. 5a) was obtained in the wet state, whilst the subsequent images were obtained every few minutes during lowering of the R.H., the last image (5f) being in the dry state. The holes observed at the surface in the dry state may correspond to regions with soluble materials which were removed during the water immersion. In Fig. 5b it can be seen that breakage of the water film occurred during scanning. Dynamic observations with fast changing formations have been videotaped.

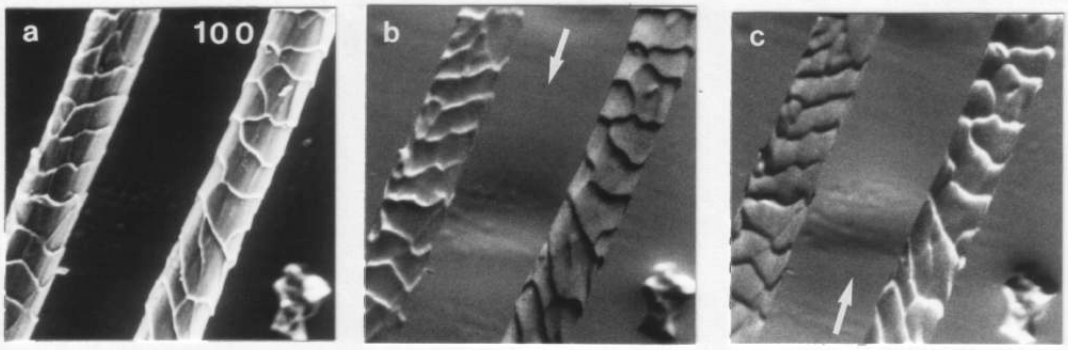

Fig. 1 Cleaned Merino wool fibres, untreated on the left and treated with alcoholic potash on the right (a) in the sum mode, (b) difference mode showing topography only of same specimens (c) opposite difference mode.

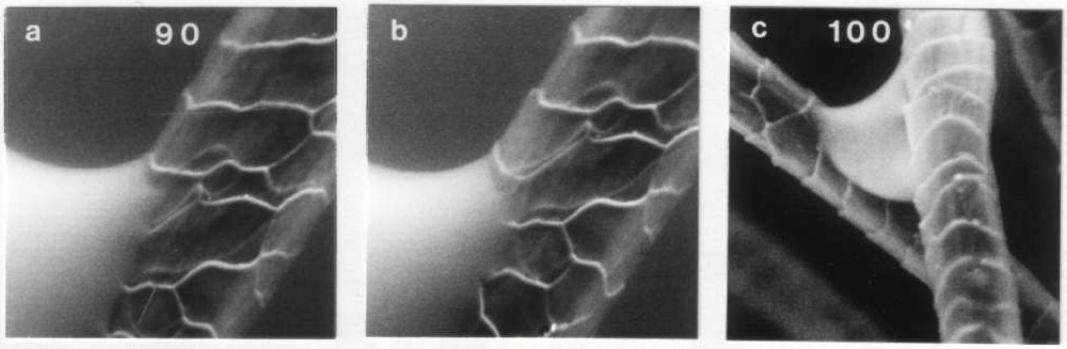

Fig. 2 (a) Cleaned Lincoln wool fibre in contact with water droplet, (b) fibre moved one scale length (c) crossed Merino fibres with water droplet.

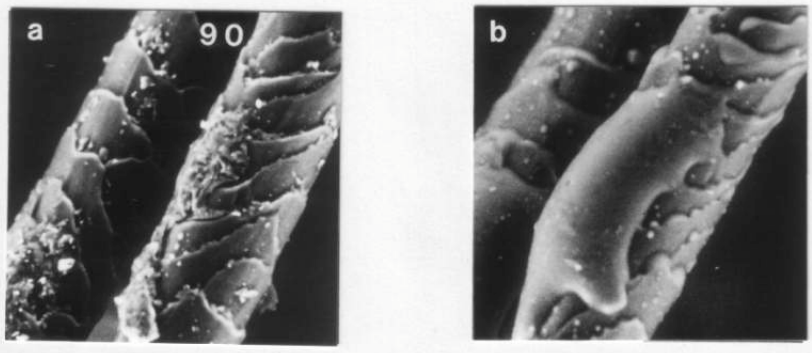

Fig. 3 Degreased Merino wool fibres (a) dry, (b) 95% R.H.

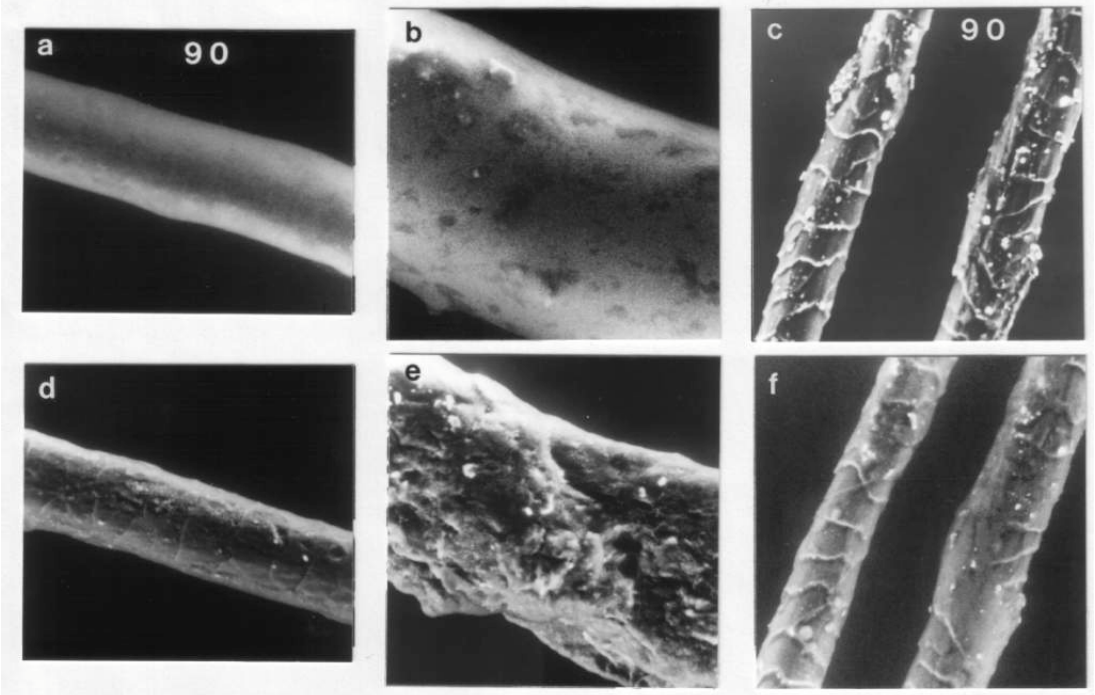

Fig. 4 Two portions of same greasy fibre (a,b) at 95% R.H. and (d,e) dry. Greasy fibres from a different lot (c) dry and (f) at 95% R.H.

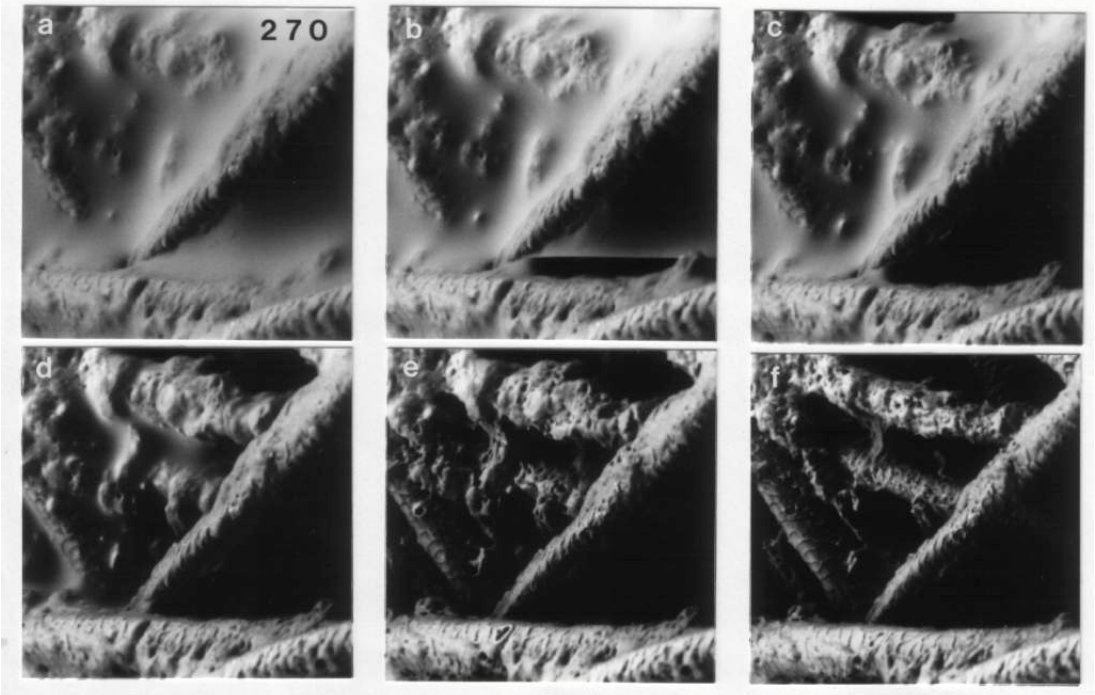

Fig. 5 Drying of greasy wool fibres (a) wet, (b,c,d,e) intermediate R.H., (f) dry.

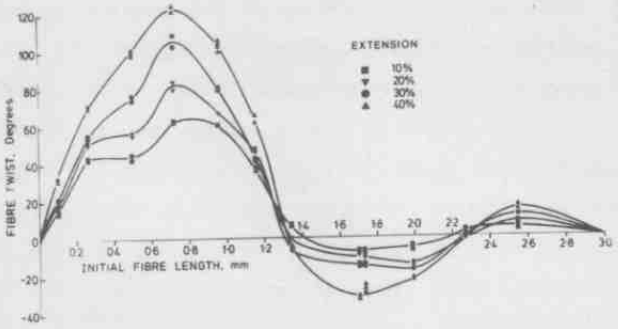

Fig. 6 Fibre twist resulting from straining to fixed extensions, plotted against the initial fibre length

3. Fibre extension

Mechanical tests and observations of the deformation of wool fibres in situ have been undertaken in the ESEM. Although it is known from light microscope observations that wool fibres twist upon extension, it is now possible to follow these changes in great detail. As a result of the high depth of focus, certain points on the fibre surface along the fibre length can be identified and the fibre twist can be measured. In Fig. 6 the twist of a Merino fibre is plotted along the initial fibre length between the two fixed ends for various overall extensions. The twist was calculated on the assumption of cylindrical cross sections. Although this assumption is not generally correct, the approximate values provide a good idea of the pronounced twist occurring along a relatively short length. This twist together with the observed uneven extension along the fibre length is now believed to be the cause for discrepancies in the measurement of Poisson ratio in the past[6,7]. With the ESEM it is now possible to monitor the uneven deformation of the surface scales and of the bulk of the fibre both longitudinally and perpendicular to the fibre axis. With the addition of a load measuring sensor on to the small extensometer, Poisson ratio measurements and the true stress-strain curve for a keratin fibre can be obtained.

4. Irradiation effects on wool

As a result of the improvement in the detection efficiency of the system, very low accelerating voltages and beam currents can be used so that the same field of view can be examined repeatedly over a period of time without any visible beam damage, thus avoiding artefacts. The exception to this is the monitoring of the wetting properties which depend crucially on the surface atomic layer of the material. In such studies the

surface properties must be studied in conjunction with the interaction with the electron beam. Conversely, the changes of the contact angle can be used to monitor radiation effects. Further, from the response of the wool fibre surface under excessive irradiation intensities, it is possible both to study the surface characteristics of the specimen [8] and to determine the limits of the technique. The capability of irradiating the natural surface of the fibre in the presence of different gases and at different pressures (plasma environment) under continuous observation has created unique possibilities in this direction. Some illustrations are given below.

A Lincoln fibre partially immersed in water is shown in Fig. 7a using 10kV and 100pA, whilst Fig. 7b shows the same fibre after exposure to 10kV, 1650pA for 5 minutes. The examples that follow illustrate the effects on Merino wool fibres irradiated on parts of the area shown as follows:

Fig. 7d,e: 5kV, 150pA, H_2 at 4 mbar, 11 mins + 20 mins
Fig. 7f : 15kV, 130pA, H_2 at 4 mbar, 17 mins
Fig. 7g : 20kV, 430pA, H_2 at 0.2 mbar, 4 mins
Fig. 7h : 20kV, 430pA, H_2 at 1.0 mbar, 4 mins
Fig. 7i : 20kV, 1550pA, Ar at 4 mbar, 10 mins
Fig. 7j : 20kV, 850pA, Ar at 4 mbar, 500 sec single frame
Fig. 7k : 15kV, 850pA, Ar at 1 mbar, 5 mins (TV).

Following the above irradiations, the images were obtained using 5kV and 150pA (in 50sec). Fig. 7c shows the initial image of a fibre whilst the same fibre is shown in Fig 7d after irradiation at two different magnifications corresponding to the white rasters (small raster 20 mins). In the topography mode of the same fibre (Fig. 7e) it is observed that a very thin layer of mass has been removed. By increasing the accelerating voltage, "bubble-like" formations appear together with some "wrinkling" (Fig. 7f). At low pressure and high voltage (Fig. 7g) a "blowing up" shape together with holes is observed. Severe loss of mass, wrinkling and bubbles result under the conditions of Fig. 7i. These phenomena occur when the scan rate during irradiation is 1 frame per second. When this rate is 500 seconds per frame, we observe a dramatic increase of density of bubbles and an equally dramatic decrease at T.V. scanning rates (Figs. 7j and k respectively).

Finally, an important finding is demonstrated in Fig. 7m. The lower portion only of the fibre shown was irradiated initially with 5kV, 350pA, at T.V. scanning rates, 0.5 mbar of argon or water vapour for 5 mins. Upon

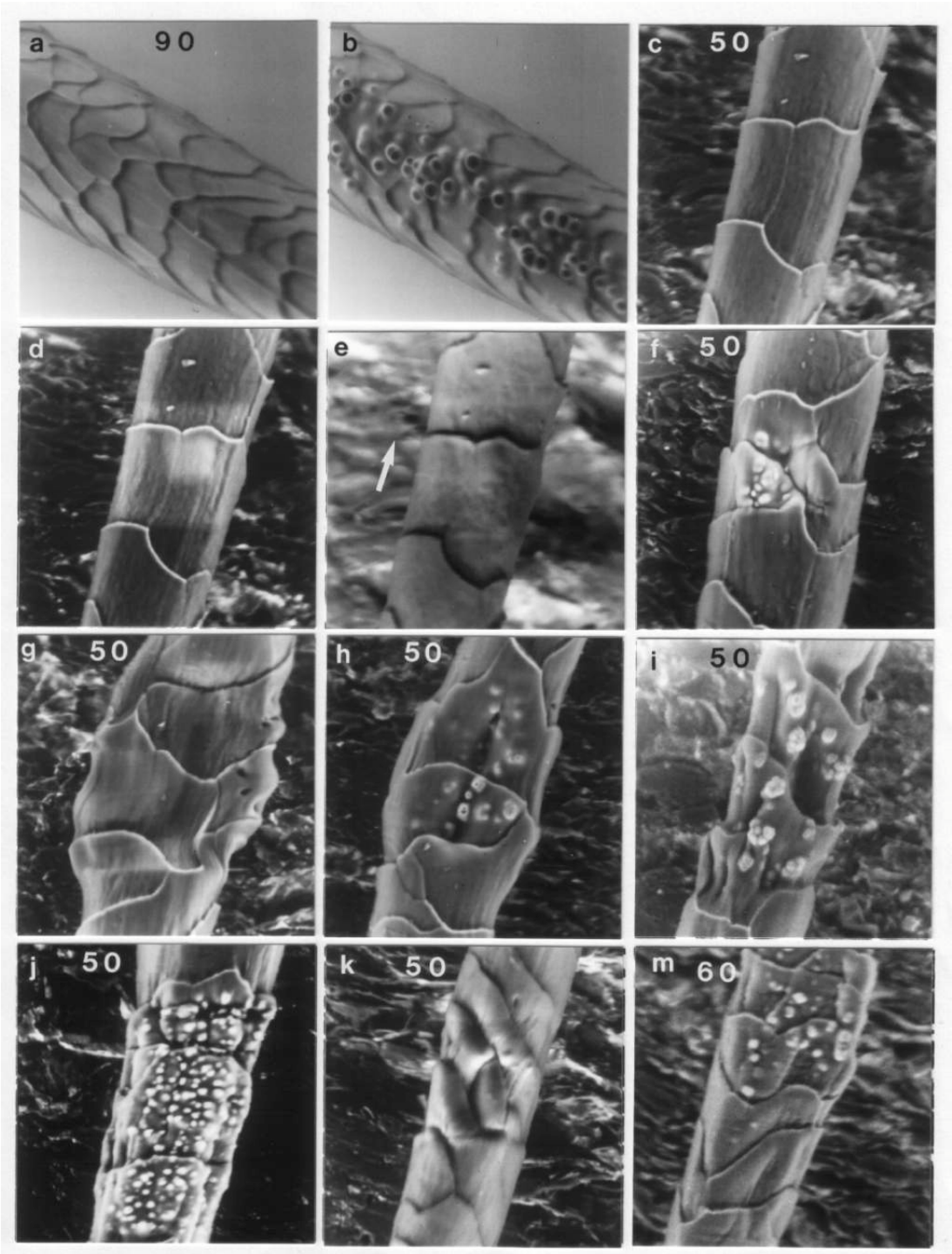

Fig. 7 Irradiation effects on Lincoln fibres (a,b) and Merino fibres (d→m) under the conditions given in text.

subsequent irradiation at 20 kV, 850pA, the lower portion does not suffer severe irradiation effects, whilst the portion above it shows bubble effects in the usual manner. Therefore, the irradiation procedure can render the fibre surface radiation-resistant in some way.

CONCLUSION

The ESEM has yielded useful results for understanding problems in wool scouring. Further, original observations on the deformation of wool fibres in situ have been performed and the mechanical properties can be studied on a new basis. Wetting of the fibres surface and irradiation studies in the ESEM have pioneered new pathways to study the wool fibre properties.

ACKNOWLEDGEMENT

This work was supported by a grant from the Wool Research Trust Fund on the recommendation of the Australian Wool Corporation. Some of the greasy fibre preparations were supplied by Dr. B.O. Bateup (CSIRO).

REFERENCES

1. G.D. Danilatos, V.N.E. Robinson and R. Postle, An environmental scanning electron microscope for studies of wet wool fibres, Proc. 6th Quinquennial Wool Textile Res. Conf., Pretoria, Vol. II, 463 (1980).
2. G.D. Danilatos, Design and construction of an atmospheric or environmental SEM (Part 1), Scanning 4, 9 (1981).
3. G.D. Danilatos and R. Postle, Design and construction of an atmospheric or environmental SEM-2, Micron 14, 41 (1983).
4. G.D. Danilatos, Design and construction of an atmospheric or environmental SEM (Part 3), Scanning 7, 26 (1985).
5. G.D. Danilatos, A gaseous detector device for an environmental SEM, Micron and Microscopica Acta 14, 307 (1983).
6. H.B. Bull, Thermal and elastic properties of α-keratin, J. Phys. Chem., 58, 101 (1954).
7. E.C. Banky and S.B. Slen, Dimensional changes and related phenomena in wool fibres under stress, Text. Res. J., 26, 204 (1956).
8. J.W. Heavens, A. Keller, J.M. Pope, D.M. Rowell, Beam-induced changes in the scanning electron microscopy of poly(oxymethylene), J. Mat. Sci. 5, 53 (1970).